Probing the Gluon Self-Interaction in Light Mesons

Christian S. Fischer[1,2] and Richard Williams[1]

[1]*Institute for Nuclear Physics, Darmstadt University of Technology, Schlossgartenstraße 9, 64289 Darmstadt, Germany*
[2]*GSI Helmholtzzentrum für Schwerionenforschung GmbH, Planckstraße 1 D-64291 Darmstadt, Germany*

(Received 20 May 2009; published 15 September 2009)

We investigate masses and decay constants of light mesons from a coupled system of Dyson-Schwinger and Bethe-Salpeter equations. We explicitly take into account dominant non-Abelian contributions to the dressed quark-gluon vertex stemming from the gluon self-interaction. We construct the corresponding Bethe-Salpeter kernel that satisfies the axial-vector Ward-Takahashi identity. Our numerical treatment fully includes all momentum dependencies with all equations solved completely in the complex plane. This approach goes well beyond the rainbow-ladder approximation and permits us to investigate the influence of the gluon self-interaction on the properties of mesons. As a first result we find indications of a nonperturbative cancellation of the gluon self-interaction contributions and pion cloud effects in the mass of the ρ meson.

DOI: 10.1103/PhysRevLett.103.122001 PACS numbers: 12.38.Lg, 11.10.St, 11.30.Rd

Introduction.—Understanding the details of the light meson spectrum from underlying QCD is still an intricate and open problem of considerable interest. Of course, pseudoscalar mesons are the (pseudo)Goldstone bosons of QCD and as such enjoy an exceptional position among the hadronic states of QCD. Within the framework of Dyson-Schwinger (DSE) and Bethe-Salpeter (BSE) equations, their Goldstone nature is retrieved in dynamical calculations provided constraints from chiral symmetry, i.e., the axial-vector Ward-Takahashi identity (AXWTI), are taken into account; see, e.g., [1,2]. However, apart from the masses of the (pseudo)Goldstone bosons all other properties of light mesons such as masses, decay constants, or charge radii are not governed by symmetry but depend on the details of the strong interaction of their constituents. This includes effects such as gluon self-interactions as well as pion cloud corrections [3].

Within the DSE-BSE framework these effects are all contained in the structure of the nonperturbative quark-gluon vertex. It is then clear that a simple rainbow-ladder parametrization of the quark-gluon interaction in terms of vector couplings cannot be sufficient to describe the wealth of phenomena associated with the internal structure of light mesons; see, e.g., [4] and references therein. In particular, a long-standing problem of the rainbow-ladder approximation is that it is too attractive, yielding masses of 800–900 MeV [5] for the axial-vector mesons.

Consequently, considerable effort has been made to go beyond the rainbow-ladder approximation. Here, Abelian corrections to the quark-gluon vertex have been considered in a number of works; see, e.g., [1,6–9]. These are, however, by far not the dominant contributions to the vertex [10]. Instead, genuinely non-Abelian diagrams including the gluon self-interaction are most important. Up to now, these have only been considered on the level of the DSE for the quark-gluon vertex and the quark propagator [10,11].

Here we provide a significant extension of these efforts. We present the first calculation of meson observables within a framework where the DSEs for the quark-gluon vertex and the quark propagator, as well as the BSE for mesons, have been coupled together without a trivialization of any momentum dependence. Furthermore, it is the first time that corrections from the dominant non-Abelian part of the quark-gluon vertex including the gluon self-interaction are tested. We determine masses and decay constants of light mesons and evaluate the influence of the gluon self-interaction corrections as compared to the rainbow-ladder approximation.

Our results are significant for $q\bar{q}$ bound states and therefore relevant for the vector mesons. In the axial-vector and scalar channels, we describe putative $q\bar{q}$ bound states which may or may not be realized in nature; see, e.g., [12]. Nevertheless, it is satisfactory that the inclusion of gluon self-interaction effects also in these channels leads to an improved description of light mesons.

Quark-gluon vertex DSE.—The fundamental dynamical quantity in the DSE-BSE approach to hadrons is the quark-gluon vertex, whose specification will ultimately determine the truncation scheme. We therefore begin with a discussion of its DSE depicted in Figs. 1(a) and 1(b). Following the detailed investigation of the quark-gluon vertex in Refs. [10,13] we approximate the full DSE [Fig. 1(a)] with the (nonperturbative) one-loop structure of Fig. 1(b). Here the first ''non-Abelian'' loop diagram in Fig. 1(b) subsumes the first two diagrams in the full DSE to first order in a skeleton expansion of the four-point functions. The two-loop diagram in the full DSE [Fig. 1(a)] is neglected. This approximation is well justified in the large and small momentum regime [10,11] and is assumed to be tractable for intermediate momenta. The remaining ''Abelian'' contributions are split into the nonresonant second loop-diagram in Fig. 1(b) and a third diagram

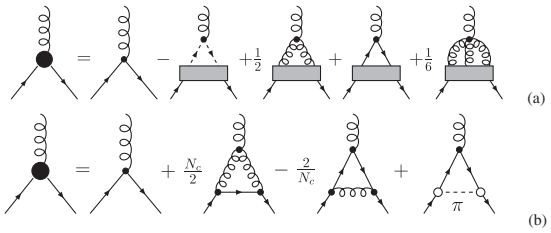

FIG. 1. The truncation employed for the quark-gluon vertex. All internal propagators are dressed, with wiggly lines indicating gluons, straight lines indicating quarks, and dashed lines indicating mesons. Open circles indicate bound-state amplitudes while solid circles represent vertex dressings. Note that the last diagram is also proportional to $1/N_c$.

containing effects due to hadron backreactions. These are dominated by the lightest hadrons, i.e., pseudoscalar mesons.

Note that the non-Abelian and nonresonant Abelian diagrams are associated with color factors $N_c/2$ and $-2/N_c$, respectively. The diagram including the pion exchange is also proportional to $1/N_c$ due to the implicit $1/\sqrt{N_c}$ dependence of the two pion amplitudes. Thus, both Abelian diagrams are suppressed by a factor of N_c^2 as compared to the non-Abelian one, a fact that is also evidenced through direct numerical calculation [10]. Consequently, these diagrams are by far not the leading ones in the vertex DSE. Moreover, as concerns meson masses, the Abelian diagrams are generally attractive. The effects of these diagrams on the mass of the ρ meson have been estimated to be about 30 MeV due to nonresonant Abelian diagrams in the quark-gluon vertex [8] with another 90 MeV due to pion cloud effects [3].

In this Letter we concentrate on the leading non-Abelian diagram in Fig. 1(b) and explore its effects on meson observables as compared to pure rainbow-ladder approximations. In order to keep our calculation tractable we employ the well-established strategy of absorbing all internal vertex dressings into effective dressing functions for the two internal gluon propagators. The resulting DSE for the quark-gluon vertex $\Gamma^\mu(p_1, p_2)$ with quark momenta p_1 and p_2 and gluon momentum p_3 reads

$$\Gamma^\mu(p_1, p_2) = Z_{1F}\gamma^\mu + \left(\frac{-iN_c}{2} g^2 Z_{1F}^2 Z_1\right) \times \int_q \{\gamma^\nu S(q)\gamma^\rho \Gamma^{3g}_{\sigma\theta\mu}(k_1, k_2) D_{\nu\sigma}(k_1) D_{\rho\theta}(k_2)\}, \tag{1}$$

with $\int_q \equiv \int \frac{d^4q}{(2\pi)^4}$, the renormalization factors Z_{1F}, Z_1, and Γ^{3g} the bare three-gluon vertex. In general, the quark-gluon vertex Γ^μ is given by a combination of 12 independent tensors built up of the quark momenta p_1^μ, p_2^μ, and γ^μ; for a detailed discussion see Ref. [10]. The dressed quark and gluon propagators are given by

$$S(p) = [-i\not{p}A(p^2) + B(p^2)]^{-1}, \tag{2}$$

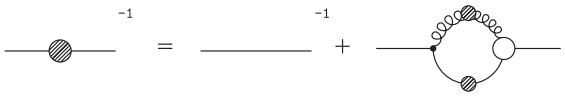

FIG. 2. The DSE for the fully dressed quark propagator.

$$D_{\mu\nu}(k) = \left(\delta_{\mu\nu} - \frac{k_\mu k_\nu}{k^2}\right)\frac{Z(k^2)}{k^2}, \tag{3}$$

where Z is the gluon dressing. The quark dressing functions A, B are determined from the DSE for the quark propagator given diagrammatically in Fig. 2. With bare quark mass m and renormalization factor Z_2 it reads

$$S^{-1}(p) = Z_2[-i\not{p} + m] + g^2 C_F Z_{1F} \int_q \gamma_\mu S(q)\Gamma_\nu(q, k) D_{\mu\nu}(k). \tag{4}$$

What remains to be specified in both the vertex and the quark DSE is the effective dressing of the gluon propagator. Here we use the momentum dependent ansatz [5]

$$Z(q^2) = \frac{4\pi}{g^2}\frac{\pi D}{\omega^2} q^4 e^{-q^2/\omega^2}, \tag{5}$$

with two parameters D and ω which provide for the scale and strength of the effective gluon interaction. Naturally, such an ansatz provides only a first step towards a full calculation of the non-Abelian diagram including input from the DSEs for the three-gluon vertex and the gluon propagator. Given that the numerical treatment of the coupled system of vertex DSE, quark DSE, and the Bethe-Salpeter equation for light mesons is somewhat involved, we defer such a calculation for future work. Nevertheless, we believe that the ansatz (5) is sufficient to provide for reliable qualitative results as concerns the effects due to the non-Abelian diagram onto meson properties. In particular, it is not sensitive to the question of scaling versus decoupling [14] in the deep infrared, $p < 50$ MeV: both scaling and decoupling lead to a combination of three-gluon vertex and gluon propagator dressings that is vanishing in the infrared in qualitative agreement with the ansatz (5). In addition, quantitative effects in the interaction below $p < 50$ MeV are not expected to affect observables in the flavor nonsinglet sector since the dynamical mass of the quark, $M \approx 350$ MeV, suppresses all physics on scales $p \ll M$ (see, however, [15]). Finally, the ansatz (5) is not sensitive to details of the Slavnov-Taylor identity (STI) for the three-gluon vertex: exactly those longitudinal parts of the vertex that are constrained from

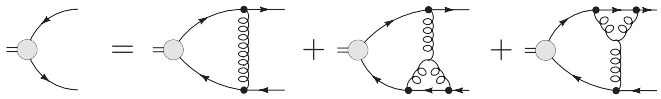

FIG. 3. The AXWTI preserving BSE corresponding to our vertex truncation. All propagators are dressed, with wiggly lines and straight lines showing gluons and quarks, respectively.

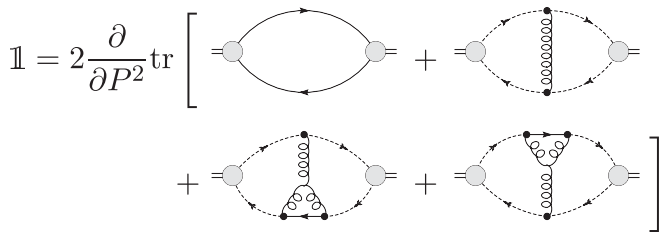

FIG. 4. Normalization of the Bethe-Salpeter amplitude. Dashed lines represent quark propagators that are kept fixed under action of the derivative.

the STI are projected out in any Landau gauge calculation by the attached transverse gluon propagators.

As concerns our numerical treatment, we solve the coupled system of quark-gluon vertex DSE and quark DSE for complex Euclidean momenta p_1 and p_2 with the ''shell method'' described in the second work of Ref. [13]. Through judicious choice of momentum routing in both the quark DSE and vertex DSE, this can be accomplished without unconstrained analytic continuation of the gluon propagator and three-gluon vertex. The BSE is solved for complex momenta by standard methods [5,16].

Bethe-Salpeter equation.—The Bethe-Salpeter amplitude $\Gamma(p;P) \equiv \Gamma^{(\mu)}(p;P)$ for a bound state of mass M is calculated through

$$[\Gamma(p;P)]_{tu} = \lambda \int_k K^{rs}_{tu}(p,k;P)[S(k_+)\Gamma(k;P)S(k_-)]_{sr}, \tag{6}$$

with $k_\pm = k \pm P/2$ and eigenvalue $\lambda(P^2 = -M^2) = 1$. The amplitude can be decomposed into at most eight Lorentz and Dirac structures constrained by transformation properties under CPT [17]. It is well known that one may construct a Bethe-Salpeter kernel K^{rs}_{tu} satisfying the AXWTI by means of a functional derivative of the quark self-energy [1,2,16,18]. Applying this cutting procedure to the quark DSE specified by Eq. (4) with the quark-gluon vertex of Eq. (2) yields the Bethe-Salpeter equation portrayed in Fig. 3 [18].

Normalization.—Since we solve the homogeneous Bethe-Salpeter equation, the correct normalization of the amplitude is achieved through an auxiliary condition [19], given pictorially in Fig. 4. This involves evaluating three-loop integrals over nonperturbative quantities, which we tackle with the aid of standard Monte Carlo techniques. Alternatively, using the eigenvalue λ in (6) and the conjugate amplitude $\bar{\Gamma}(k,-P) = C\Gamma(-k,-P)C^{-1}$ one may use the equivalent normalization condition [20]

$$\left(\frac{d\ln(\lambda)}{dP^2}\right)^{-1} = \mathrm{tr}\int_k 3\bar{\Gamma}(k,-P)S(k_+)\Gamma(k,P)S(k_-). \tag{7}$$

This requires significantly less numerical effort and can be simply applied to all truncations of the BSE.

We will see that the diagrams of Fig. 4 beyond the impulse approximation give large corrections of the order of 30%. This is important for observables calculated from the amplitudes such as leptonic decay constants [16].

Results.—Table I details the results of our truncation scheme, including gluon self-interaction effects in all 12 tensor structures of the quark-gluon vertex, compared to the rainbow-ladder approximation with only vector-vector interactions. The model parameters ω and D were tuned such that for the latter we obtain reasonable pion observables, and the quark mass is fixed at 5 MeV. We do not fit observables for our beyond the rainbow-ladder truncation scheme since the inclusion of additional resonant and nonresonant corrections would require further parameter tuning.

In all cases the non-Abelian corrections are seen to have only a small impact on the mass of the pion, though the decay constant is enhanced from 94 MeV to about 110 MeV. This shift is comparable in size to the negative one of the order of 10 MeV [3] induced by pion could effects, i.e., the third loop diagram in Fig. 1(b). We also investigated the impact of the Abelian, second loop diagram in 1(b) without use of the real-axis approximation made in [8]. We confirm that the change in the pion mass is negligible for their preferred value of $G = 0.5$ and find a small reduction of $\sim$2 MeV in the decay constant. Once all corrections are combined, we expect significant cancella-

TABLE I. Masses and decay constants for a variety of mesons, calculated using rainbow-ladder (R-L) and our beyond-the-rainbow (BTR) truncation. Decay constants are determined from the full normalization condition, except those indicated by a caret where only the leading term of the impulse approximation is used. Masses and decay constants are given in MeV.

Model	ω	D	m_π	f_π	$\hat{f}_\pi$	m_ρ	f_ρ	$\hat{f}_\rho$	m_σ	m_{a_1}	m_{b_1}
R-L	0.50	16	138	94	$\cdots$	758	154	$\cdots$	645	926	912
BTR			138	111	(127)	881	176	(181)	884	1055	972
R-L	0.48	20	138	95	$\cdots$	763	154	$\cdots$	676	937	895
BTR			141	112	(129)	887	176	(181)	886	1040	946
R-L	0.45	25	136	92	$\cdots$	746	149	$\cdots$	675	917	858
BTR			142	110	(128)	873	173	(177)	796	1006	902
Experiment [21]			138	92.4	$\cdots$	776	156	$\cdots$	400–1200	1230	1230

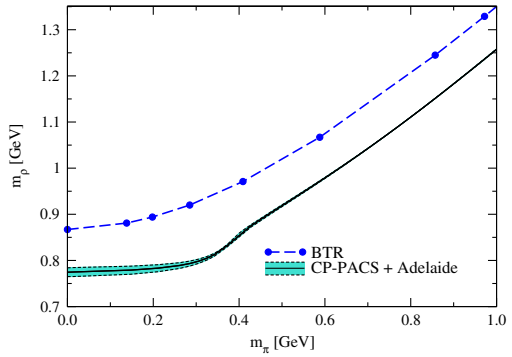

FIG. 5 (color online). ρ mass as a function of the pion mass (BTR) compared to an extrapolation (CP-PACS + Adelaide) based on (corrected) lattice data; Ref. [22].

tions such that the mass and decay constant of the pion are close to the experimental value.

For the ρ meson, including the gluon self-interaction enhances its mass by $\sim$120 MeV compared to the pure rainbow-ladder approximation, with the decay constant increased by $\sim$20 MeV. This is an intriguing result since it has long been suspected that corrections beyond the rainbow-ladder approximation cancel among themselves in the vector channel [1,6]. Indeed, the resonant and nonresonant contributions from the Abelian diagrams in 1(b) are known to provide reductions of the ρ mass of $\sim$90 and 30 MeV, respectively [3,8]. Similar cancellations happen for the decay constant. We therefore see for the first time strong evidence of this nonperturbative cancellation mechanism. This is one of the main results of this Letter.

Figure 5 shows the ρ mass as a function of the pion mass for our truncation beyond the rainbow (BTR) compared to a chiral extrapolation based on (corrected) lattice data; Ref. [22]. Because of the discussion above we expect the explicit inclusion of the resonant and nonresonant Abelian contributions in our BTR scheme to move our results close to the lattice data.

For completeness, we also report the masses of the scalar and axial vectors in Table I. In all cases we see an enhancement compared to the rainbow-ladder approximation.

Conclusions.—We presented an exploratory study of light mesons using a sophisticated truncation of the Bethe-Salpeter equations beyond the rainbow-ladder approximation, in which we consider the gluon self-interaction contributions to the quark-gluon vertex. Close to the chiral limit we obtain masses for the ρ meson of $\sim$900 MeV, consistent with extrapolations from quenched lattice simulations. There is evidence that the subsequent inclusion of pion cloud effects and nonresonant contributions to the quark-gluon interaction brings the ρ mass back to its physical value, thus supporting a long suspected nonperturbative cancellation mechanism. Our truncation provides for a well-founded setup to further explore the details of the nonperturbative quark-gluon interaction and gluon self-interaction effects in mesons. In this respect it is complementary to the one very recently suggested in Ref. [23].

We thank Pete Watson for discussions. This work was supported by the Helmholtz Young Investigator Grant VH-NG-332 and the Helmholtz International Center for FAIR within the LOEWE program of the State of Hesse.

[1] A. Bender, C. D. Roberts, and L. Von Smekal, Phys. Lett. B **380**, 7 (1996).
[2] H. J. Munczek, Phys. Rev. D **52**, 4736 (1995).
[3] C. S. Fischer and R. Williams, Phys. Rev. D **78**, 074006 (2008).
[4] G. Eichmann *et al.*, Phys. Rev. C **77**, 042202 (2008).
[5] R. Alkofer, P. Watson, and H. Weigel, Phys. Rev. D **65**, 094026 (2002).
[6] A. Bender *et al.*, Phys. Rev. C **65**, 065203 (2002).
[7] M. S. Bhagwat *et al.*, Phys. Rev. C **70**, 035205 (2004).
[8] P. Watson, W. Cassing, and P. C. Tandy, Few-Body Syst. **35**, 129 (2004); P. Watson and W. Cassing, Few-Body Syst. **35**, 99 (2004).
[9] H. H. Matevosyan, A. W. Thomas, and P. C. Tandy, Phys. Rev. C **75**, 045201 (2007).
[10] R. Alkofer *et al.*, Ann. Phys. (N.Y.) **324**, 106 (2009).
[11] M. S. Bhagwat and P. C. Tandy, Phys. Rev. D **70**, 094039 (2004).
[12] C. Amsler and N. A. Tornqvist, Phys. Rep. **389**, 61 (2004); M. Wagner and S. Leupold, Phys. Rev. D **78**, 053001 (2008).
[13] C. S. Fischer, D. Nickel, and J. Wambach, Phys. Rev. D **76**, 094009 (2007); C. S. Fischer, D. Nickel, and R. Williams, Eur. Phys. J. C **60**, 1434 (2008).
[14] C. S. Fischer, A. Maas, and J. M. Pawlowski, arXiv:0810.1987 [Ann. Phys. (N.Y.) (to be published)].
[15] R. Alkofer, C. S. Fischer, and R. Williams, Eur. Phys. J. A **38**, 53 (2008).
[16] P. Maris and C. D. Roberts, Phys. Rev. C **56**, 3369 (1997).
[17] C. H. Llewellyn-Smith, Ann. Phys. (N.Y.) **53**, 521 (1969).
[18] P. Maris and P. C. Tandy, Nucl. Phys. B, Proc. Suppl. **161**, 136 (2006).
[19] R. E. Cutkosky and M. Leon, Phys. Rev. **135**, B1445 (1964).
[20] N. Nakanishi, Phys. Rev. **138**, B1182 (1965).
[21] C. Amsler *et al.* (Particle Data Group), Phys. Lett. B **667**, 1 (2008).
[22] C. R. Allton *et al.*, Phys. Lett. B **628**, 125 (2005).
[23] L. Chang and C. D. Roberts, Phys. Rev. Lett. **103**, 081601 (2009).